

Role of Metal-Dependent Regulation of ESX-3 Secretion in Intracellular Survival of *Mycobacterium tuberculosis*

Emir Tinaztepe,^a Jun-Rong Wei,^{b*} Jenelle Raynowska,^a Cynthia Portal-Celhay,^a Victor Thompson,^a Jennifer A. Philips^{a*}

Division of Infectious Diseases, Department of Medicine, New York University School of Medicine, New York, New York, USA^a; Department of Immunology and Infectious Diseases, Harvard T. H. Chan School of Public Health, Boston, Massachusetts, USA^b

More people die every year from *Mycobacterium tuberculosis* infection than from infection by any other bacterial pathogen. Type VII secretion systems (T7SS) are used by both environmental and pathogenic mycobacteria to secrete proteins across their complex cell envelope. In the nonpathogen *Mycobacterium smegmatis*, the ESX-1 T7SS plays a role in conjugation, and the ESX-3 T7SS is involved in metal homeostasis. In *M. tuberculosis*, these secretion systems have taken on roles in virulence, and they also are targets of the host immune response. ESX-3 secretes a heterodimer composed of EsxG (TB9.8) and EsxH (TB10.4), which impairs phagosome maturation in macrophages and is essential for virulence in mice. Given the importance of EsxG and EsxH during infection, we examined their regulation. With *M. tuberculosis*, the secretion of EsxG and EsxH was regulated in response to iron and zinc, in accordance with the previously described transcriptional response of the *esx-3* locus to these metals. While iron regulated the *esx-3* expression in both *M. tuberculosis* and *M. smegmatis*, there is a significant difference in the dynamics of this regulation. In *M. smegmatis*, the *esx-3* locus behaved like other iron-regulated genes such as *mbtB*. In *M. tuberculosis*, both iron and zinc modestly repressed *esx-3* expression. Diminished secretion of EsxG and EsxH in response to these metals altered the interaction of *M. tuberculosis* with macrophages, leading to impaired intracellular *M. tuberculosis* survival. Our findings detail the regulatory differences of *esx-3* in *M. tuberculosis* and *M. smegmatis* and demonstrate the importance of metal-dependent regulation of ESX-3 for virulence in *M. tuberculosis*.

The intracellular pathogen *Mycobacterium tuberculosis* survives within phagocytic immune cells such as macrophages and dendritic cells (1). *M. tuberculosis* evades degradation by the endolysosomal pathway, growing in an early endosome-like compartment or escaping into the cytosol (2, 3). Acidified lysosomes are just one obstacle for the bacilli to overcome as the host also regulates metals such as iron, zinc, copper, and manganese to create an uninhabitable microenvironment (4). These metals are essential but at the same time can be toxic, so both host and pathogen tightly regulate them. For example, macrophages can increase zinc levels in *M. tuberculosis*-containing phagosomes to induce toxicity (5). Calprotectin, on the other hand, is released at sites of infection to bind and withhold zinc and manganese from bacteria (6). Similarly, host iron is bound to glycoproteins such as transferrin and lactoferrin, and during infection the host further limits available iron by reducing plasma iron levels via ferroportins (7–9). In addition, lipocalin 2-mediated sequestration of iron has been shown to be an important antimycobacterial innate immune response (10). To compete for iron, *M. tuberculosis* produces siderophores, mycobactin and carboxymycobactin, which are high-affinity iron chelators (11). Since iron is a strong redox catalyst that can be toxic to cells, *M. tuberculosis* stores excess iron in complex with ferritin (BfrB) (12). In addition to being a metabolic necessity, iron can also affect virulence through other means, such as ferric uptake regulator A (FurA)-modulated resistance to H₂O₂ and susceptibility to the antimicrobial drug isoniazid (13, 14). Thus, in order to survive over the course of an infection, *M. tuberculosis* has to appropriately respond to a range of concentrations of metals.

In mycobacteria, the iron-dependent regulator (IdeR), the zinc uptake repressor (Zur), and, as recently shown, manganese transport regulator (MntR) control gene expression in response to iron, zinc, and manganese, respectively. Analysis of the IdeR, Zur,

and MntR regulons demonstrated that the *esx-3* locus, which encodes the ESX-3 type 7 secretion system (T7SS), is transcriptionally regulated by iron, zinc, and manganese (15–17). ESX-3 is required for the utilization of iron from mycobactin in both nonpathogenic *Mycobacterium smegmatis* and in *M. tuberculosis*, although the mechanism by which ESX-3 promotes iron acquisition is not understood (18–20). In *M. tuberculosis*, ESX-3 is essential under standard laboratory conditions; growth can be restored to *esx-3* mutants by the addition of exogenous mycobactin (20). *M. smegmatis* tolerates the deletion of *esx-3*, since it can also scavenge iron using the siderophore exochelin, which is absent in *M. tuberculosis*, as well as obtaining ferric iron through porins (21, 22). The transcriptional regulation of *esx-3* also differs between *M. smegmatis* and *M. tuberculosis*. Although IdeR transcriptionally re-

Received 7 March 2016 Returned for modification 4 April 2016

Accepted 19 May 2016

Accepted manuscript posted online 31 May 2016

Citation Tinaztepe E, Wei J-R, Raynowska J, Portal-Celhay C, Thompson V, Philips JA. 2016. Role of metal-dependent regulation of ESX-3 secretion in intracellular survival of *Mycobacterium tuberculosis*. *Infect Immun* 84:2255–2263. doi:10.1128/IAI.00197-16.

Editor: S. Ehrt, Weill Cornell Medical College

Address correspondence to Jennifer A. Philips, jphilips@dom.wustl.edu.

* Present address: Jun-Rong Wei, Novartis Institutes for Biomedical Research, Emeryville, California, USA; Jennifer A. Philips, Division of Infectious Diseases, Department of Medicine and Department of Molecular Microbiology, Washington University School of Medicine, St. Louis, Missouri, USA.

Supplemental material for this article may be found at <http://dx.doi.org/10.1128/IAI.00197-16>.

Copyright © 2016, American Society for Microbiology. All Rights Reserved.

presses *esx-3* in response to iron in both species, *esx-3* is not transcriptionally regulated by zinc in *M. smegmatis* (18).

ESX-3 is required for secretion of EsxG, EsxH, and two pairs of PE-PPE proteins (18, 20). EsxG (Tb9.8) and EsxH (Tb10.4), which form a heterodimer (18, 23), are highly immunogenic and therefore investigated as vaccine candidates (24–26). A vaccine study utilizing an *M. smegmatis* strain that lacked the endogenous *esx-3* locus and instead contained the *M. tuberculosis* *esx-3* locus found that it protected against subsequent *M. tuberculosis* infection in mice (27). Tufariello et al. recently demonstrated that *esxG* and *esxH* are required for *M. tuberculosis* to grow in mice. Interestingly, *esxG* and *esxH* play a role in virulence beyond their requirement for iron acquisition (20). Consistent with these findings, we previously showed that the EsxG–EsxH complex from *M. tuberculosis*, but not that from the *M. smegmatis* EsxG–EsxH complex, targets the host hepatocyte growth factor-regulated tyrosine kinase substrate (Hrs), a component of the endosomal sorting complexes required for transport (ESCRT) (28). *M. tuberculosis* EsxG–EsxH inhibits ESCRT, which is required for phagosome maturation. Accordingly, we found that an additional episomal copy of *esxG-esxH* introduced into wild-type *M. tuberculosis* enhances the ability of the bacilli to impair phagosome maturation. This suggested that the levels of EsxG and EsxH are important for host interactions and that the endogenous levels are limiting when the bacilli are grown *in vitro*.

We reasoned that iron and zinc might alter *M. tuberculosis* virulence by virtue of regulating expression of *esxG* and *esxH*. For example, if iron and zinc fully repress *esx-3*, then microenvironments within the host that are rich in iron and zinc might attenuate the bacilli. At the same time, since EsxG and EsxH are dominant T-cell antigens, diminished expression might allow individual bacilli to evade immune responses during the course of infection and also might compromise the efficacy of an EsxG- or EsxH-based vaccine. To better define the relative contribution of iron and zinc to the expression of the *esx-3* locus, we directly examined how these metals influence transcription and secretion of EsxG and EsxH in *M. tuberculosis* compared to *M. smegmatis*. We then examined the role of metal-regulated expression of *esx-3* in the intracellular survival of *M. tuberculosis*.

MATERIALS AND METHODS

Bacterial strains and growth conditions. Wild-type *M. tuberculosis* (H37Rv), *M. tuberculosis* Δ *esxH* (mc²7846) (20), wild-type *M. smegmatis* (mc²155), *M. smegmatis* Δ *esx-3*, and *M. smegmatis* Δ *esx-3::esx-3*_{Mtb} strains were grown in Middlebrook 7H9 medium supplemented with 10% oleic acid-albumin-dextrose-catalase (OADC), 0.05% Tween 80, and 0.2% glycerol. The *esxG-esxH* complementing plasmid (pJP130), described below, was selected with 25 μ g of kanamycin/ml. For iron and zinc starvation experiments, bacteria were grown in liquid Middlebrook 7H9 medium to logarithmic phase and then subcultured in chelated Sauton's (CS) medium (0.5 g of KH₂PO₄, 2 g of citric acid monohydrate, 4 g of asparagine, 1 g of MgSO₄, 60 ml of glycerol, and 0.05% Tween 80 per liter). After the pH was adjusted to 7.4, Sauton's medium was chelated using 10 g of Chelex 100 (Sigma) over 2 days, after which 1 g of MgSO₄ was added back. FeCl₃ (50 μ M) or ZnSO₄ (3 μ M) was added as a sterile solution prior to bacterial inoculation. *M. tuberculosis* strains grown in 7H9 were transferred to CS medium supplemented with iron and zinc as indicated at an optical density at 600 nm (OD₆₀₀) of \sim 0.2 and grown for 3 or 6 days, at which point they were washed twice with phosphate-buffered saline and subcultured into their respective growth media for one more day prior to sample collection. *M. smegmatis* strains grown in 7H9

were subcultured in CS medium supplemented with iron and zinc at an OD₆₀₀ of \sim 0.2 and grown for \sim 9 h prior to sample collection.

Strain and plasmid construction. The *M. smegmatis* Δ *esx-3::esx-3*_{Mtb} strain was generated by inserting pJM-TBesx3(Kan-L5), an integrated plasmid, with *M. tuberculosis* *esx-3* (*esx-3*_{Mtb}) into the chromosomal L5 integration site of the *M. smegmatis* Δ *esx-3* strain (18). In the first step, we used recombineering (29) to generate pJM-TBesx3, which contains the entire *esx-3* locus, extending from 433 bp before the start codon of Rv0208 until the end of Rv0292. *Escherichia coli* was transformed with the cosmid clone 4-68, which contains the *M. tuberculosis* genomic regions of *esx-3*, and pKD119 (30), the arabinose-inducible recombinase plasmid. This strain was grown at 30°C, induced by arabinose, and prepared as electro-competent cells. PCR was performed using pJM1 (31) as the template with the primer pair TBesx3JMF and TBesx3JMR (see Table S1 in the supplemental material). The PCR product was digested with DpnI and transformed into the prepared competent cells and selected on 25 μ g of chloramphenicol/ml at 30°C. pJM-TBesx3 was verified by sequencing the entire *esx-3* locus. We then replaced the chloramphenicol acetyltransferase gene with L5 integrase-attP, together with *aph*, again by recombineering to form pJM-TBesx3(Kan-L5). PCR product Kan-L5 that contains L5 integrase-attP, together with *aph*, was amplified by using template plasmid pMC1s (32) and the primer pair Int-Ab-F and Int-Ab-R (see Table S1 in the supplemental material). The *E. coli* strain containing pKD119 and pJM-TBesx3 was grown at 30°C, induced by arabinose, transformed the DpnI-digested Kan-L5, and then selected on 50 μ g of kanamycin/ml at 37°C. pJM-TBesx3(Kan-L5) was verified by sequencing. pJM-TBesx3(Kan-L5) was then transformed into the *M. smegmatis* Δ *esx-3* strain to form the *M. smegmatis* Δ *esx-3::esx-3*_{Mtb} strain.

The *esxG-esxH* complementing plasmid (pJP130) contains *esxG-esxH-espG₃*, pJP130 was constructed by inserting *espG₃* (Rv0289) into pYUB1944, which contains *esxG-esxH* under the control of the *hsp60* promoter (as described previously [20]). Rv0289 was amplified from *M. tuberculosis* genomic DNA by PCR using forward (TAGAAGCTTCTCG CGCTACATGGATGC) and reverse (CCAATCGATTACGAGGATTG GGTGG) primers, digested with HindIII, and cloned into the HindIII site after Rv0288 in pYUB1944. The addition of Rv0289 to pYUB1944 resulted in enhanced secretion of EsxG and EsxH compared to the parent plasmid.

Bacterial protein preparation and Western blotting. To prepare samples for Western blotting, bacteria were pelleted, and culture supernatants were filtered through a 0.22- μ m-pore-size filter. Culture filtrate (CF) proteins were precipitated overnight at 4°C using 10% trichloroacetic acid. The protein precipitate was washed with acetone, air dried, and resuspended in sodium dodecyl sulfate (SDS) sample buffer. Bacterial pellets were lysed by bead beating in lysis buffer (50 mM Tris-HCl, 5 mM EDTA, 0.6% SDS, 10 mM NaH₂PO₄, 1 \times Halt protease inhibitor [Thermo Fisher Scientific]) with 0.1-mm zirconia/silica beads (Biospec Products, Inc.). Samples were boiled at 95°C for 5 min prior to SDS-PAGE. Protein extracts were separated by SDS-PAGE, transferred onto nitrocellulose membranes, and probed with α EsxG–EsxH rabbit antisera (20) or α Ag85 rabbit antisera (generously provided by the J. D. Ernst lab [33]). Proteins were detected with horseradish peroxidase-conjugated goat anti-rabbit IgG antibody (1:10,000; Life Technologies) and visualized with the Amersham ECL reagent (GE Healthcare). Quantification of band intensities was performed using ImageJ software.

Recombinant EsxG–EsxH production and immunoblotting. EsxG_{Mt} and EsxH_{Mt} were expressed in tandem as a single polypeptide separated by a linker (GLVPRGSTG) as previously described (28). To make EsxG_{Ms}–EsxH_{Ms}, Genewiz synthesized the full-length coding regions of EsxG_{Ms} and EsxH_{Ms} separated by a linker region that is identical to that in the EsxG_{Mt}–EsxH_{Mt} plasmid in pUC57. The EsxG_{Ms}–EsxH_{Ms} coding region was moved from pUC57 to pET22b on an NdeI–XhoI fragment. *E. coli* [BL21(DE3); Invitrogen] transformed with the EsxG_{Mt}–EsxH_{Mt} or EsxG_{Ms}–EsxH_{Ms} expression plasmid was grown in Luria broth at 37°C to an OD₆₀₀ of 0.7 and then induced with 450 μ M IPTG (isopropyl- β -D-thiogalactopyranoside; Promega) for 3 h, harvested by centrifugation at

4°C, and frozen at -80°C. Pellets were later resuspended in lysis buffer (300 mM NaCl, 50 mM NaH₂PO₄, 1× Halt protease inhibitor cocktail [Thermo Fisher Scientific] supplemented with 10 mM imidazole [Fisher BioReagents], 3 U of benzonase nuclease [Novagen]/ml, and 1 mg of lysozyme [Sigma-Aldrich]/ml at pH 8.0) and incubated at room temperature for 40 min, followed by centrifugation at 10,000 × g for 30 min at 4°C. The supernatant was incubated with nickel-nitrilotriacetic acid (Ni-NTA) Superflow resin (Qiagen) at 4°C for 1.5 h. The Ni-NTA resin was washed with lysis buffer containing up to 60 mM imidazole, followed by elution in lysis buffer containing 250 mM imidazole. Thrombin (Novagen) was added (1 U/ml) overnight at room temperature to cleave the linker connecting EsxG and EsxH. To remove thrombin, the samples were diluted in lysis buffer at a final concentration of 10 mM imidazole and rebound to Ni-NTA resin, washed, and eluted with 250 mM imidazole. The purity and the extent of thrombin cleavage were assessed by SDS-gel electrophoresis and Coomassie blue staining. Proteins were quantified with a NanoDrop 1000 using ultraviolet absorbance of 280 nm and/or by comparison to bovine serum albumin standards on a Coomassie gel.

Quantitative reverse transcription (RT)-PCR analysis. For total RNA extraction, pellets were lysed by bead beating 5 OD₆₀₀ units of each sample in 1 ml of TRIzol (Life Technologies) three times for 1 min. RNA was precipitated according to the manufacturer's instructions, resuspended in RNase-free water, and stored at -80°C. DNase-treated (DNase I, amplification grade; Life Technologies) RNA samples were used as the templates for cDNA synthesis (Superscript III reverse transcriptase; Life Technologies) and treated with RNase prior to amplification. The expression of *mbtI*, *bfrB*, *esxG*, and *ppe4* were determined by using real-time PCR. Each sample was amplified using SYBR green (Roche Life Science) according to the manufacturer's protocol. Each cycle consisted of denaturation at 95°C for 15 s, annealing at 59.5°C for 5 s, and extension at 72°C for 15 s. 16S rRNA and *dnaA* were used for the normalization for *M. tuberculosis* and *M. smegmatis*, respectively. The primers used are listed in Table S1 in the supplemental material.

Intracellular bacterial growth assay. Murine bone marrow-derived macrophages (BMDMs) were obtained and infected with a single cell suspension of *M. tuberculosis* at a multiplicity of infection of 3 as previously described (28). Extracellular bacteria were washed away at 4 h. At the indicated times, BMDMs were lysed with 0.2% Triton X-100, and serial dilutions were plated on Middlebrook 7H10 solid medium containing 200 ng of mycobactin J (Allied Monitor, Inc.)/ml.

Statistical analysis. To assess statistical significance, differences between groups were analyzed by Student *t* test. We considered a *P* value below 0.05 to be statistically significant.

RESULTS

***M. tuberculosis* EsxG-EsxH secretion and iron regulation are impaired in the *M. smegmatis* Δ *esx-3::esx-3*_{Mtb} strain.** Previously, we found that *M. tuberculosis* EsxG and EsxH are not secreted when they are expressed in *M. smegmatis* (28). To examine whether *M. tuberculosis* EsxG and EsxH can be secreted by *M. smegmatis* if the entire *M. tuberculosis* *esx-3* locus is provided, we compared secretion profiles from three strains: wild-type *M. smegmatis* (mc²155), *M. smegmatis* lacking *esx-3* (Δ *esx-3*), and *M. smegmatis* lacking *esx-3* but containing *M. tuberculosis* *esx-3* (Δ *esx-3::esx-3*_{Mtb}). This strain is similar to the published vaccine strain (27), so analyzing its EsxG-EsxH secretion profile was also of interest. We transferred mid-log-phase cultures grown in 7H9 medium into Sauton's medium with or without iron and analyzed secretion after 9 h of growth. We examined the secretion of EsxG and EsxH using antisera from rabbits immunized with purified recombinant *M. tuberculosis* EsxG-EsxH complex. In wild-type *M. smegmatis*, endogenous EsxG-EsxH was present in culture filtrate (CF) and undetectable in the pellet fraction. In contrast, we detected a large amount of *M. tuberculosis* EsxG-EsxH in the pellet

fraction of the *M. smegmatis* Δ *esx-3::esx-3*_{Mtb} strain and only a minor fraction in the CF (Fig. 1A), suggesting an incompatibility between the *M. tuberculosis* ESX-3 machinery and *M. smegmatis* resulting in impaired secretion. Our antibody recognizes *M. tuberculosis* EsxG and EsxH much better than it recognizes *M. smegmatis* EsxG and EsxH, which are 70% identical to the *M. tuberculosis* homologues (Fig. 1B). Therefore, the amount of endogenous EsxG-EsxH secreted by mc²155 shown on the Western blot is >10-fold higher than the amount of *M. tuberculosis* EsxG-EsxH secreted from the Δ *esx-3::esx-3*_{Mtb} strain. In addition, the amount of *M. smegmatis* EsxG-EsxH in the CF of mc²155 noticeably decreased with the addition of iron, as expected. In contrast, we were surprised to find that the abundance of *M. tuberculosis* EsxG-EsxH in both the pellet and the CF from the Δ *esx-3::esx-3*_{Mtb} strain was unaffected by the addition of iron. In accordance with this finding, quantitative reverse transcription-PCR (qRT-PCR) analysis showed that whereas expression of the endogenous *esxG* locus in *M. smegmatis* was induced 200-fold in the absence of iron, *M. tuberculosis* *esxG* in the Δ *esx-3::esx-3*_{Mtb} strain was unaffected by the addition of iron (Fig. 1C).

Because the Δ *esx-3::esx-3*_{Mtb} strain failed to repress *esxG* in response to iron, we examined its ability to repress *mbtI*. Interestingly, in contrast to the wild-type strain and the Δ *esx-3* mutant, the Δ *esx-3::esx-3*_{Mtb} strain failed to strongly repress *mbtI* in response to iron (Fig. 1D). This suggests that the Δ *esx-3::esx-3*_{Mtb} strain is defective in iron sensing, uptake, or utilization. In addition, although all strains were inoculated comparably, the endpoint ODs showed that the *M. smegmatis* strain containing *M. tuberculosis* ESX-3 grew less well in liquid medium (Fig. 1E), showing that the presence of *M. tuberculosis* ESX-3 and perhaps the accumulation of intracellular *M. tuberculosis* EsxG-EsxH impair iron regulation and is detrimental to the growth of *M. smegmatis*.

Iron and zinc modestly regulate the expression of the *M. tuberculosis* *esx-3* locus. To examine the transcriptional response of the *esx-3* locus to iron in *M. tuberculosis* itself, we first examined how long it took the growth of *M. tuberculosis* to slow down when mid-log-phase cultures were transferred from 7H9 into Sauton's medium without FeCl₃. Since *M. tuberculosis* can store excess iron in ferritin, it was not surprising that for the first 3 days after transfer, *M. tuberculosis* grew equivalently irrespective of the presence of iron; growth diverged by the fourth day (Fig. 2A). To examine the transcriptional response of the *esx-3* locus to iron and zinc, we harvested RNA for qRT-PCR analysis after 3 days of growth in CS medium with or without FeCl₃ and ZnSO₄ (50 and 3.67 μM, respectively). The *esx-3* locus in *M. tuberculosis* extends from *rv0282* to *rv0292*, with Zur and IdeR binding sites located upstream of *eccA*₃ (*rv0282*) (34) and at least one additional internal promoter located upstream of *esxG* (*rv0287*) (16) (see Fig. S1 in the supplemental material). We analyzed expression of *ppe4* (*rv0286*) and *esxG*, along with two other IdeR-regulated genes, *mbtI* and *bfrB*, which are encoded outside the *esx-3* locus. *mbtI* encodes isochorismate synthase, a salicylate synthase required for mycobactin production that is repressed by iron-bound IdeR. On the other hand, *bfrB*, which encodes an *M. tuberculosis* ferritin that stores intracellular iron, belongs to a small subset of genes that are induced by IdeR (34, 35). As expected, the expression of *mbtI* was repressed 3-fold by the presence of iron and unaffected by zinc, whereas *bfrB* was induced 2.7-fold by iron and also unaffected by zinc (Fig. 2B). In contrast, *esxG* and *ppe4* showed minimal response to iron. When zinc was absent, iron repressed *ppe4* 1.6-fold

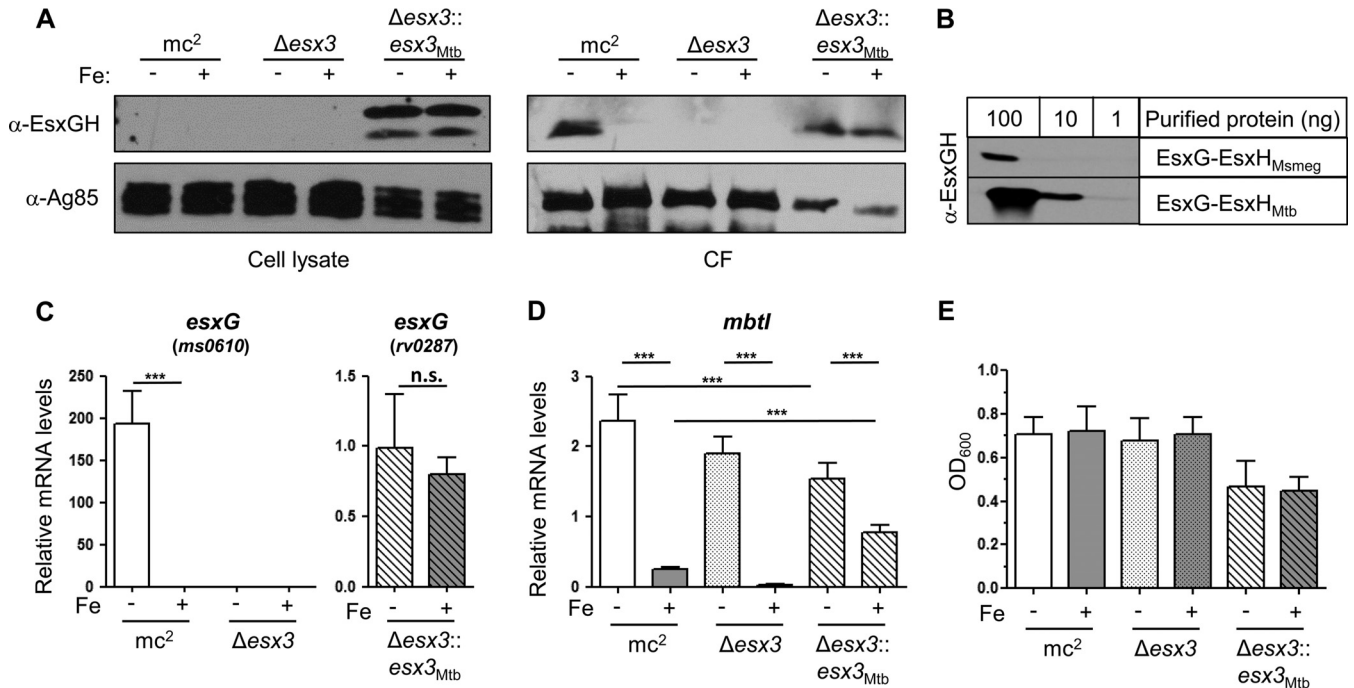


FIG 1 Analysis of *M. tuberculosis* ESX-3 expressed in *M. smegmatis*. (A, C to E) Wild-type (*mc*²155), Δ *esx-3*, and Δ *esx-3*::*esx-3*_{Mtb} *M. smegmatis* strains were subcultured from 7H9 into in CS medium with ZnSO₄ and with or without iron as indicated for 9 h. (A) EsxG-EsxH and Ag85b were analyzed by Western blotting of cell lysates and CFs. (B) Anti-EsxG-EsxH Western blot of purified recombinant EsxG-EsxH_{Msmeg} and EsxG-EsxH_{Mtb}. (C and D) The mRNA levels of *esxG* (C) and *mbtI* (D) were normalized to *dnaA*. In panel C, *ms0610*-specific primers were used for *mc*²155 and Δ *esx-3* strains, and *rv0287*-specific primers were used for the Δ *esx-3*::*esx-3*_{Mtb} strain. Data represent the means \pm the standard errors of the mean (SEM) from three experiments with six technical replicates each. ***, $P < 0.001$ (unpaired Student *t* test). n.s., not significant. (E) OD₆₀₀ measurements from two experiments after equal inocula were subcultured for 9 h as indicated. Data represent the means \pm the SEM.

($P = 0.0002$), whereas it repressed expression of *esxG* only 1.3-fold ($P = 0.025$). When zinc was included in the media, iron again only modestly repressed *ppe4* and *esxG*, resulting in 1.3- and 1.7-fold reductions in transcript, respectively (Fig. 2B). The addition of zinc resulted in an ~ 2 -fold inhibition of *esxG* and *ppe4* expression both in the presence and in the absence of iron. 7H9, a standard laboratory medium for *M. tuberculosis* that contains approximately 150 μ M iron and 6 μ M zinc, repressed *esxG* and *ppe4* to a similar level as had CS medium supplemented with 50 μ M iron and 3.67 μ M zinc.

To determine whether a longer duration of iron starvation would result in more dramatic changes in *esx-3* expression, we compared cells grown in the presence or absence of iron for 6 days (Fig. 2B). *mbtI* and *bfrB* exhibited 25-fold repression and 22-fold induction, respectively, compared to the ~ 3 -fold differences seen after 3 days. This difference was largely attributable to more complete inhibition of expression in the repressing condition for both genes. For *esxG* and *ppe4*, iron and zinc individually again only yielded modest differences. Thus, the expression of *esx-3* is only minimally responsive to iron, irrespective of the presence of zinc, in contrast to the dynamic regulation of other IdeR-regulated genes in *M. tuberculosis*. Likewise, zinc modestly repressed *esxG* and *ppe4*, with ~ 2 -fold repression at both the 3- and the 6-day time points (15). Overall, at both time points, the combined effect of iron and zinc together resulted in an approximately 3- to 6-fold decrease in expression of *esx-3* relative to growth in deficient media. Notably, in the 6-day samples, *esxG* and *ppe4* were dramatically more repressed in 7H9 than Sauton's medium containing

both iron and zinc, which may reflect trace manganese in 7H9 (17). This suggests that when experiments are performed on bacteria grown in 7H9, they are likely to reflect relatively low levels of ESX-3-secreted effectors.

Because free iron had a limited effect on *esx-3* expression, we tested heme, which *M. tuberculosis* can also utilize as an iron source (36). We found that when *M. tuberculosis* was transferred from 7H9 into Sauton's medium containing up to 100 μ M hemin, this delivered an increasingly toxic dose of iron to *M. tuberculosis* (Fig. 2C). At sublethal doses, hemin strongly repressed *mbtI* ~ 30 -fold, but *esxG* showed just a 2-fold difference, similar to the response to FeCl₃ (Fig. 2D). Even at toxic doses, where *mbtI* was repressed ~ 100 -fold, *esxG* showed just a 2-fold inhibition. Thus, although ESX-3 is required for the acquisition of iron from mycobactin, it is not completely repressed, even in toxic doses of iron, in contrast to what is observed for the mycobactin biosynthetic pathway. Instead, multiple metals individually appear to make a modest contribution to *esx-3* regulation, as suggested by prior studies (19, 34, 37). This is quite distinct from the regulation of *M. smegmatis* *esx-3*, which displays a level of iron responsiveness comparable to that of the IdeR-regulated genes *mbtI* and *bfrB* (Fig. 3).

Secretion of *M. tuberculosis* ESX-3 substrates is regulated by iron and zinc. Siegrist et al. previously examined the effect of iron on the secretion of EsxH from *M. smegmatis* and BCG using EsxH fused to myc, which was expressed under the control of the *hsp60* promoter (18). To determine whether the transcriptional changes we observed correlated with secretion differences, we examined the secretion of endogenous EsxG and EsxH from *M. tuberculosis*

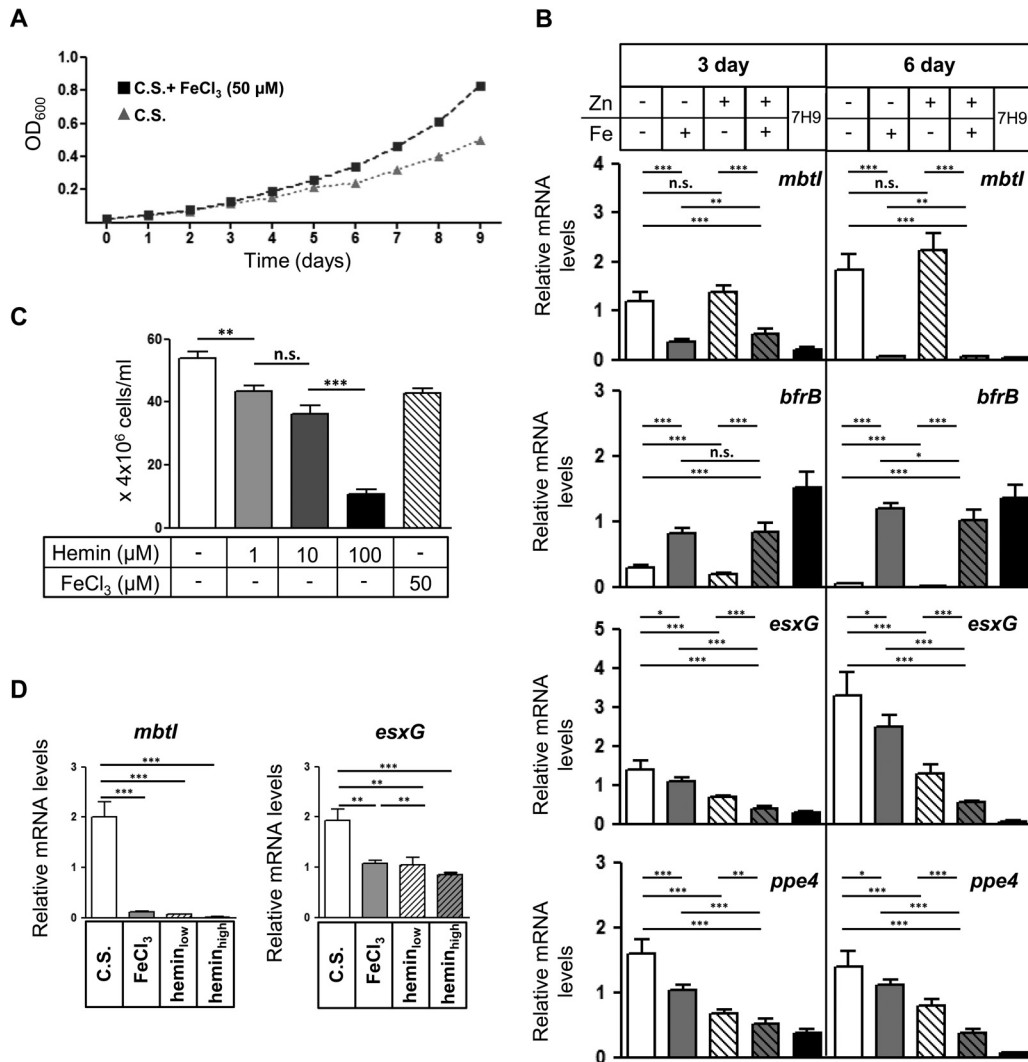


FIG 2 Iron and zinc modestly repress expression of the *M. tuberculosis* *esx-3* locus. (A) OD₆₀₀ measurements of *M. tuberculosis* subcultured in chelated Sauton’s medium (C.S.) with or without iron (3.67 μM ZnSO₄ present in both conditions). (B) *M. tuberculosis* was grown in 7H9 or CS containing iron (FeCl₃) or zinc (ZnSO₄) as indicated for 3 or 6 days. The mRNA levels of *mbtI*, *bfrB*, *esxG*, and *ppe4* were normalized to 16S rRNA and are shown as fold changes compared to the sample without iron or zinc. Data represent the means ± the SEM from three experiments with five technical replicates each. (C) *M. tuberculosis* was subcultured from 7H9 into CS medium without hemin or with increasing concentrations of hemin (1, 10, and 100 μM) or iron (50 μM) as indicated for 24 h, and bacterial CFU were enumerated. Data represent the means ± the SEM from one experiment with six technical replicates. (D) *M. tuberculosis* was grown in CS medium without iron supplementation or with hemin (low, 3 μM; high, 30 μM) or FeCl₃ (50 μM) for 1 week. The mRNA levels of *mbtI* and *esxG* were normalized to 16S rRNA. Data represent the means ± the SEM from one experiment with five technical replicates. *, P < 0.05; **, P < 0.01; ***, P < 0.001 (unpaired Student *t* test). n.s., not significant.

using the antibody raised against the EsxG-EsxH complex (20). Initially, we analyzed CF after 2 or 6 days of incubation in Sauton’s medium with or without iron, and we did not detect an effect of iron on the level of secreted EsxG and EsxH. We reasoned that the initial amount of EsxG and EsxH secreted might mask differences that occur as the cells adapt over time, particularly given the modest transcriptional effects that we observed. Therefore, in subsequent experiments, after bacteria grew in Sauton’s medium for either 3 or 6 days under iron replete or depleted conditions, they were subcultured again under their respective conditions for an additional 24 h and the proteins secreted into the CF during this 24-h period were analyzed by Western blotting (Fig. 4A). Using ImageJ software, we quantified the intensity of EsxG-EsxH on Western blots from three independent experiments and normal-

ized to Ag85, which is secreted by the twin arginine translocator system and partitions in both the cell pellet and the CF (Fig. 4B) (38). We did not detect any EsxG-EsxH associated with the bacterial pellet, suggesting that *M. tuberculosis* secretes nearly all of the EsxG-EsxH that is produced. After 3 days of growth in media lacking iron and zinc, there was no difference in the EsxG-EsxH protein levels in CF compared to cells grown with iron. The addition of zinc alone caused an ~4-fold decrease in secretion (P = 0.0148), which was further boosted to an ~11-fold decrease by the addition of iron (P = 0.0009). When CF was analyzed from bacteria subcultured after 6 days of growth in distinct iron and zinc conditions, there was more experimental variability than seen after 3 days, but the overall trend was the same (Fig. 4C and D). Consistent with the expression data, EsxG-EsxH production was

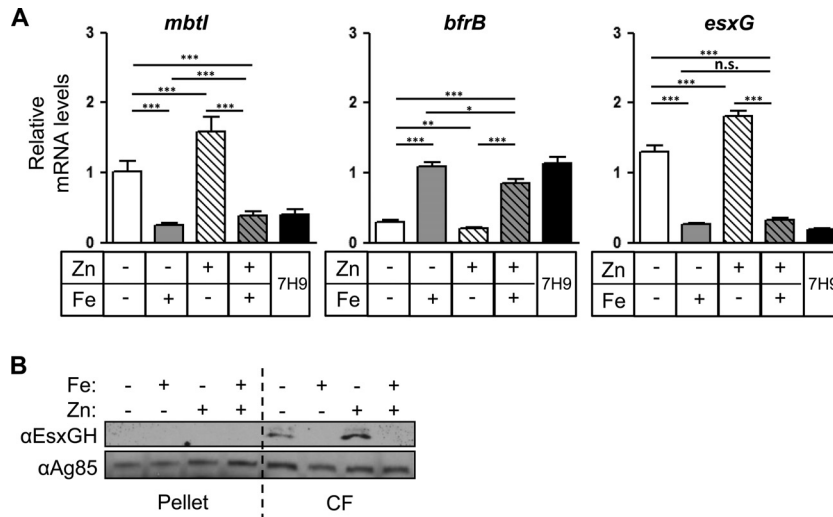


FIG 3 Iron regulates expression and secretion of EsxG-EsxH in *M. smegmatis*. (A and B) *M. smegmatis* was grown in 7H9 or CS medium containing iron or zinc as indicated for 9 h. (A) The relative mRNA levels of *mbtI*, *bfrB*, and *esxG* were normalized to *dnaA* and are shown as fold changes compared to the sample without iron or zinc. Data represent the means \pm the SEM from two experiments with six technical replicates each. *, $P < 0.05$; **, $P < 0.01$; ***, $P < 0.001$ (unpaired Student *t* test). n.s., not significant. (B) EsxG-EsxH and Ag85 complex proteins were analyzed by Western blotting of cell lysates and CFs.

never completely suppressed. Overall, analysis of EsxG-EsxH protein secretion shows general concordance with the transcriptional analysis. This, along with the absence of an intracellular pool of EsxG-EsxH, suggests that iron and zinc do not also posttranscriptionally regulate EsxG-EsxH secretion. When we grew *M. smegmatis* in the presence or absence of iron and zinc for 9 h and collected proteins from both the bacterial pellet and the CF (Fig. 3B), even though we collected CF proteins after a single transfer into CS medium, we found that secreted EsxG-EsxH was clearly diminished by the addition of iron. Thus, as for the transcriptional

response, the secretion of EsxG-EsxH in *M. smegmatis* is highly responsive to iron, whereas *M. tuberculosis* *esx-3* modestly responds to both metals and is not fully repressed even in the presence of both iron and zinc.

Iron- and zinc-mediated repression of *esx-3* decreases *M. tuberculosis* survival in macrophages. Over the course of infection, *M. tuberculosis* can exist in various environments and thus is exposed to a wide range of metals (39–41). In order to determine whether iron- and zinc-mediated regulation of EsxG and EsxH might influence virulence, we infected murine BMDMs with *M.*

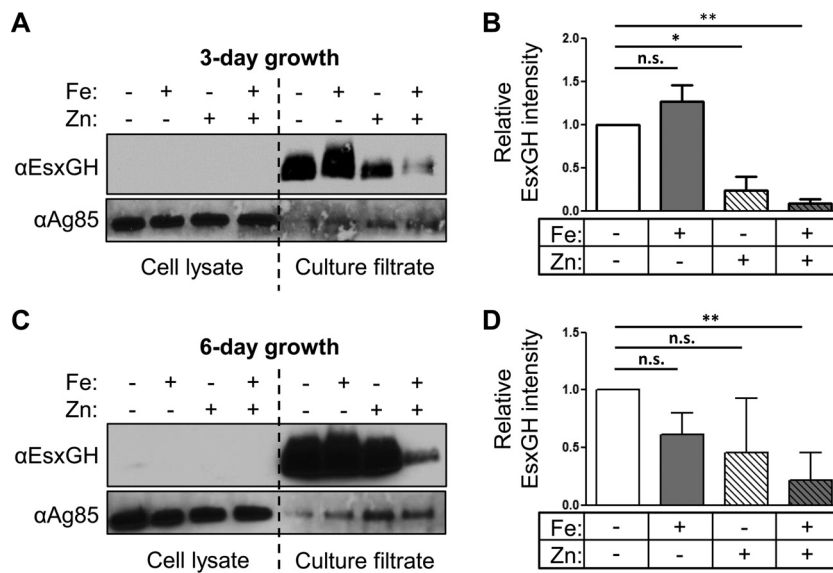


FIG 4 Iron and zinc inhibit secretion of *M. tuberculosis* EsxG-EsxH. (A to D) *M. tuberculosis* was grown in C.S. containing iron (FeCl_3) or zinc (ZnSO_4) as indicated. (A and C) EsxG-EsxH and Ag85 complex proteins were analyzed by Western blotting of cell lysates and CFs after 3-day (A) and 6-day (C) treatments. Long exposures of the CF are shown to demonstrate the presence of EsxG-EsxH in media containing both iron and zinc. (B and D) EsxG-EsxH protein levels in CF were quantified from three independent experiments using ImageJ software and normalized to Ag85. Data represent the means \pm the SEM. *, $P < 0.05$; **, $P < 0.01$ (unpaired Student *t* test). n.s., not significant.

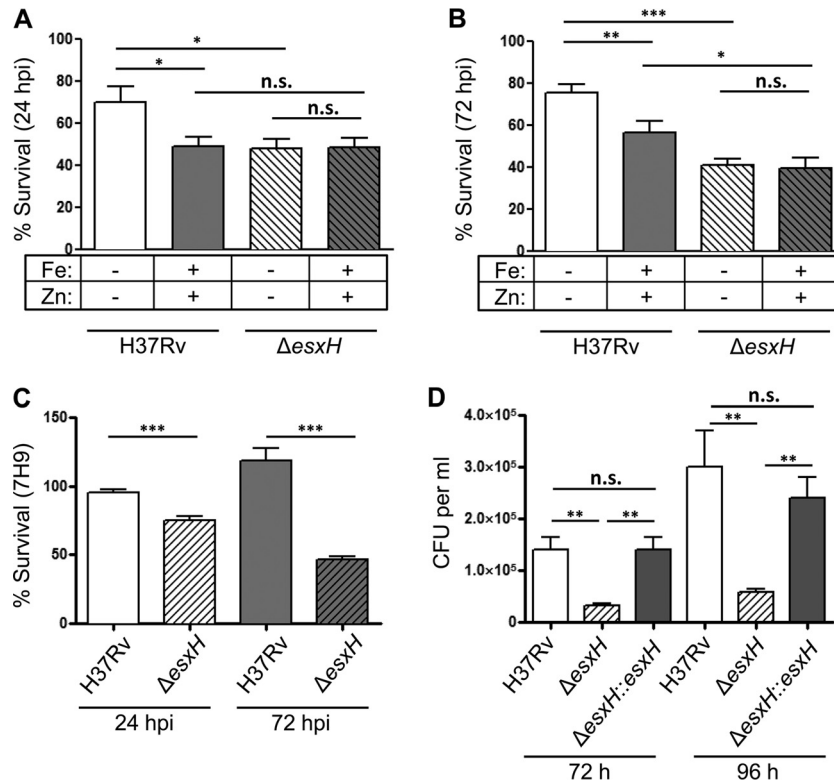


FIG 5 Iron- and zinc-mediated suppression of EsxH impair intracellular survival. BMDMs were infected with *M. tuberculosis* that had been pregrown for 3 days in CS medium containing iron or zinc as indicated (A and B) or in 7H9 (C and D) at a multiplicity of infection of 3. (A to C) CFU were enumerated at 4, 24, and 72 hpi, and data are expressed as the percent bacterial survival at 24 hpi (CFU at 24 hpi/CFU at 4 hpi) \pm the SEM and 72 hpi (CFU at 72 hpi/CFU at 4 hpi) \pm the SEM from three experiments, with five experimental replicates each. (D) BMDMs were infected with wild-type *M. tuberculosis*, Δ esxH, and Δ esxH::esxH strains, and the CFU were enumerated 72 and 96 hpi from five replicates. *, $P < 0.05$; **, $P < 0.01$; ***, $P < 0.001$ (unpaired Student *t* test). n.s., not significant.

tuberculosis that was pregrown for 3 days in Sauton's medium with iron and zinc or without iron and zinc to test conditions that maximize the difference in EsxG-EsxH secretion. We anticipated that once inside cells, bacteria pregrown under both conditions would eventually achieve similar levels of expression, so we assessed the intracellular survival over the first 24 h of infection. We noticed that *M. tuberculosis* pregrown in Sauton's medium (either with or without iron and zinc) were impaired intracellularly relative to bacteria pregrown in 7H9 (compare Fig. 5A and B to Fig. 5C). In addition, we found that wild-type *M. tuberculosis* (H37Rv) grown in iron- and zinc-depleted Sauton's medium prior to infection displayed modestly higher survival in BMDMs than *M. tuberculosis* grown in iron- and zinc-replete Sauton's medium (Fig. 5A). These differences were still apparent at 72 h postinfection (hpi) (Fig. 5B). To distinguish whether the enhanced intracellular survival of *M. tuberculosis* grown in iron- and zinc-depleted conditions was mediated by EsxH, as opposed to an effect of the numerous other genes with altered expression or some physiological consequence of growing without iron and zinc, we examined an Δ esxH mutant, which fails to secrete both EsxG and EsxH (20). At 24 hpi, the Δ esxH mutant had impaired intracellular survival, similar to wild-type *M. tuberculosis* grown in the presence of iron and zinc, where little EsxG-EsxH is secreted. Moreover, iron and zinc did not affect the intracellular survival of the Δ esxH mutant at either 24 or 72 hpi (Fig. 5A and B). Overall, these findings are consistent with the idea that the secretion of EsxG-EsxH, which is maximal in low-iron and -zinc conditions, assists in bacterial sur-

vival during the initial interaction with macrophages. Thus, although growth of *M. tuberculosis in vitro* is improved by iron and zinc, the initial intracellular growth is impaired, which may be explained at least in part by the repression of *esxG* and *esxH*. Because the transcription of *esx-3* was repressed to similar levels when *M. tuberculosis* strains were grown in 7H9 or CS medium with iron and zinc for 3 days, we also compared the intracellular survival rates of Rv and Δ esxH strains in BMDMs after pregrowth in 7H9. There was a mild difference in intracellular survival of the Δ esxH mutant compared to wild-type bacilli at 24 hpi; this difference became more pronounced by 72 hpi and could be complemented by a plasmid encoding *esxG-esxH* (Fig. 5C and D). Thus, although the secretion of EsxG-EsxH is likely to be relatively low in 7H9, it still contributes to the intracellular survival of *M. tuberculosis*.

DISCUSSION

Recent work has highlighted that *M. tuberculosis* ESX-3 and its secreted effectors, EsxG and EsxH, play a role in virulence beyond their previously recognized role in iron acquisition (20, 28). In addition, they are major immune targets of the host (24–26). Given the importance of these molecules during infection, we examined the relative contribution of iron and zinc to the expression and secretion of EsxG and EsxH. As expected, we found that both metals regulated the *M. tuberculosis esx-3* locus. However, *ppe4* and *esxG* exhibited only modest differences in expression in response to iron or zinc. In contrast, the dynamics of *esx-3* expression in *M. smegmatis* mirrored the results seen with other iron-

responsive genes. The differences in the amount of secreted EsxG and EsxH reflected the transcriptional regulation of the *esx-3* locus. Since we performed these studies, manganese has also been shown to regulate expression of *esx-3* (17). The additional repression of *esx-3* seen after prolonged culturing in 7H9 compared to iron- and zinc-replete conditions may reflect the presence of trace manganese, although other differences in the media or growth rate may play a role as well.

We also monitored the regulation of *M. tuberculosis* ESX-3 when the locus was integrated into an *M. smegmatis* strain lacking its endogenous *esx-3* locus. Analysis of EsxG and EsxH by Western blotting showed that the majority of the protein remained cell associated and was not secreted into the CF. One possibility is that the *M. tuberculosis* ESX-3 secretion apparatus does not assemble properly in *M. smegmatis*. Alternatively, there may be proteins that are required to assist in EsxG-EsxH recognition by ESX-3 that are encoded outside the locus. In addition, we found that expression of the *M. tuberculosis* locus was not iron-regulated when introduced into *M. smegmatis*. The IdeR binding sites differ between *M. tuberculosis* and *M. smegmatis* by two nucleotides (see Fig. S1 in the supplemental material). Thus, one possibility is that the *M. smegmatis* IdeR protein does not recognize the binding site in the *M. tuberculosis* promoter or that the spacing relative to the transcriptional start site, which differs in the two species, is not optimal. Alternatively, there may be an aberrant transcriptional start site at the ectopic locus of integration. However, a different possibility is raised by our observations that the presence of *M. tuberculosis* ESX-3 also affected iron-mediated repression of the endogenous *mbtI* gene. In wild-type *M. smegmatis*, *mbtI* was repressed 9.5-fold by the addition of iron, but in the *M. smegmatis* $\Delta esx-3::esx-3_{Mtb}$ strain *mbtI* expression was only repressed 2-fold (Fig. 1D). This difference reflects both lower expression in the absence of iron and diminished repression by iron in the $\Delta esx-3::esx-3_{Mtb}$ strain. Thus, one possibility is that the accumulation of Esx-3 substrates in the $\Delta esx-3::esx-3_{Mtb}$ strain impairs iron sensing or iron utilization or that the diminished iron responsiveness is a consequence of the attenuated growth in culture.

In order to determine whether iron- and zinc-mediated regulation of EsxG and EsxH affect bacterium-host interactions, we infected BMDMs with bacteria pregrown in media with or without iron and zinc. We found that bacterial survival was enhanced by pregrowth under conditions that maximized EsxG-EsxH secretion. Consistent with the idea that the effect of zinc and iron is mediated by differences in EsxG-EsxH secretion, these metals had no effect on the intracellular survival of the $\Delta esxH$ strain. Thus, the early interactions of *M. tuberculosis* with macrophages depend upon metals in the medium prior to infection, likely at least in part by virtue of altering EsxG and EsxH abundance, although it is also possible these effects are mediated by effectors that are cosecreted with EsxG and EsxH (20). Although it is not possible to measure the secretion of EsxG and EsxH by *M. tuberculosis* growing in standard 7H9, given the transcriptional repression that we observed of *esx-3*, we predict that there would be low levels of EsxG and EsxH secreted. This has important implications for studies of *M. tuberculosis* grown *in vitro* and subsequently used for infections. Although extremely low levels of EsxG and EsxH are sufficient to allow *M. tuberculosis* to utilize iron (20, 42), such restricted expression is unlikely to reflect the situation *in vivo* and may be limiting in terms of the interactions with macrophages. Moreover, these results suggest that the zinc and iron concentra-

tions in distinct host microenvironments would create bacterial heterogeneity in ESX-3 function that might have important consequences in terms of pathogenesis and immune responses. Although decreased EsxH expression might be a way to evade prominent T cell-mediated immune responses, this would likely come at the cost of diminished fitness *in vivo*.

During the evolution of environmental mycobacteria to pathogenicity, the *esx-3* locus acquired an upstream Zur binding site, resulting in zinc-dependent regulation that is lacking in the saprophytic relative. This adaptation presumably reflects the specific environments of *M. tuberculosis* in the host. For example, studies have shown very high levels of zinc inside mycobacterial phagosomes (43). In addition, ESX-3 has acquired additional functions in the obligate pathogen that are not present in *M. smegmatis*. We speculate that the altered transcriptional regulation of the locus in *M. tuberculosis* also reflects its importance in virulence. Recent studies, along with this one, demonstrate that the ESX-3 secretion system plays an important role in host-pathogen interaction due to its role in both metal homeostasis and virulence. Understanding how ESX-3 contributes to pathogenesis may enable novel strategies that can subvert this system and promote *M. tuberculosis* clearance.

ACKNOWLEDGMENTS

We thank members of the J. Philips, J. Ernst (NYU School of Medicine), and H. Darwin (NYU School of Medicine) laboratories for assistance, and we thank S. Koster (NYU), E. Rubin (HSPH), M. Rodriguez (Rutgers), and J. Tufariello (Albert Einstein College of Medicine) for helpful discussions and comments on the manuscript. We thank J. Tufariello and W. Jacobs, Jr. (Albert Einstein College of Medicine), for providing the *esxH* mutant.

FUNDING INFORMATION

This work, including the efforts of Jennifer Philips, Emir Tinaztepe, and Victor Thompson, was funded by NIH, NIAID (R01 AI087682). This work, including the efforts of Cynthia Portal-Celhay, was funded by NIH, NIAID (K08 AI119150-01).

REFERENCES

1. Wolf AJ, Linas B, Trevejo-Nunez GJ, Kincaid E, Tamura T, Takatsu K, Ernst JD. 2007. *Mycobacterium tuberculosis* infects dendritic cells with high frequency and impairs their function in vivo. *J Immunol* 179:2509–2519. <http://dx.doi.org/10.4049/jimmunol.179.4.2509>.
2. Philips JA, Ernst JD. 2012. Tuberculosis pathogenesis and immunity. *Annu Rev Pathol* 7:353–384. <http://dx.doi.org/10.1146/annurev-pathol-011811-132458>.
3. Stanley SA, Cox JS. 2013. Host-pathogen interactions during *Mycobacterium tuberculosis* infections. *Curr Top Microbiol Immunol* 374:211–241. http://dx.doi.org/10.1007/82_2013_332.
4. Neyrolles O, Wolschendorf F, Mitra A, Niederweis M. 2015. Mycobacteria, metals, and the macrophage. *Immunol Rev* 264:249–263. <http://dx.doi.org/10.1111/imr.12265>.
5. Botella H, Peyron P, Levillain F, Poincloux R, Poquet Y, Brandli I, Wang C, Tailleux L, Tilleul S, Charrière GM, Waddell SJ, Foti M, Lugo-Villarino G, Gao Q, Maridonneau-Parini I, Butcher PD, Castagnoli PR, Gicquel B, de Chastellier C, Neyrolles O. 2011. Mycobacterial P1-type ATPases mediate resistance to zinc poisoning in human macrophages. *Cell Host Microbe* 10:248–259. <http://dx.doi.org/10.1016/j.chom.2011.08.006>.
6. Damo SM, Kehl-Fie TE, Sugitani N, Holt ME, Rathi S, Murphy WJ, Zhang Y, Betz C, Hensch L, Fritz G, Skaar EP, Chazin WJ. 2013. Molecular basis for manganese sequestration by calprotectin and roles in the innate immune response to invading bacterial pathogens. *Proc Natl Acad Sci U S A* 110:3841–3846. <http://dx.doi.org/10.1073/pnas.1220341110>.
7. Cassat JE, Skaar EP. 2013. Iron in infection and immunity. *Cell Host Microbe* 13:509–519. <http://dx.doi.org/10.1016/j.chom.2013.04.010>.
8. Nemeth E, Tuttle MS, Powelson J, Vaughn MB, Donovan A, McVey Ward D, Ganz T, Kaplan J. 2004. Hepcidin regulates cellular iron efflux

- by binding to ferroportin and inducing its internalization. *Science* 306: 2090–2093.
9. Van Zandt KE, Sow FB, Florence WC, Zwilling BS, Satoskar AR, Schlesinger LS, Lafuse WP. 2008. The iron export protein ferroportin 1 is differentially expressed in mouse macrophage populations and is present in the mycobacterial-containing phagosome. *J Leuk Biol* 84:689–700. <http://dx.doi.org/10.1189/jlb.1107781>.
 10. Saiga H, Nishimura J, Kuwata H, Okuyama M, Matsumoto S, Sato S, Matsumoto M, Akira S, Yoshikai Y, Honda K, Yamamoto M, Takeda K. 2008. Lipocalin 2-dependent inhibition of mycobacterial growth in alveolar epithelium. *J Immunol* 181:8521–8527. <http://dx.doi.org/10.4049/jimmunol.181.12.8521>.
 11. Fang Z, Sampson SL, Warren RM, Gey van Pittius NC, Newton-Foot M. 2015. Iron acquisition strategies in mycobacteria. *Tuberculosis* 95: 123–130. <http://dx.doi.org/10.1016/j.tube.2015.01.004>.
 12. Pandey R, Rodriguez GM. 2014. IdeR is required for iron homeostasis and virulence in *Mycobacterium tuberculosis*. *Mol Microbiol* 91:98–109. <http://dx.doi.org/10.1111/mmi.12441>.
 13. Zahrt TC, Song J, Siple J, Deretic V. 2001. Mycobacterial FurA is a negative regulator of catalase-peroxidase gene katG. *Mol Microbiol* 39: 1174–1185. <http://dx.doi.org/10.1111/j.1365-2958.2001.02321.x>.
 14. Pym AS, Domenech P, Honore N, Song J, Deretic V, Cole ST. 2001. Regulation of catalase-peroxidase (KatG) expression, isoniazid sensitivity, and virulence by furA of *Mycobacterium tuberculosis*. *Mol Microbiol* 40: 879–889. <http://dx.doi.org/10.1046/j.1365-2958.2001.02427.x>.
 15. Maciag A, Dainese E, Rodriguez GM, Milano A, Provvedi R, Pasca MR, Smith I, Palu G, Riccardi G, Manganelli R. 2007. Global analysis of the *Mycobacterium tuberculosis* Zur (FurB) regulon. *J Bacteriol* 189:730–740. <http://dx.doi.org/10.1128/JB.01190-06>.
 16. Maciag A, Piazza A, Riccardi G, Milano A. 2009. Transcriptional analysis of ESAT-6 cluster 3 in *Mycobacterium smegmatis*. *BMC Microbiol* 9:48. <http://dx.doi.org/10.1186/1471-2180-9-48>.
 17. Pandey R, Russo R, Ghanny S, Huang X, Helmann J, Rodriguez GM. 2015. MntR(Rv2788): a transcriptional regulator that controls manganese homeostasis in *Mycobacterium tuberculosis*. *Mol Microbiol* 98:1168–1183. <http://dx.doi.org/10.1111/mmi.13207>.
 18. Siegrist MS, Unnikrishnan M, McConnell MJ, Borowsky M, Cheng TY, Siddiqi N, Fortune SM, Moody DB, Rubin EJ. 2009. Mycobacterial Esx-3 is required for mycobactin-mediated iron acquisition. *Proc Natl Acad Sci U S A* 106:18792–18797. <http://dx.doi.org/10.1073/pnas.0900589106>.
 19. Serafini A, Boldrin F, Palu G, Manganelli R. 2009. Characterization of a *Mycobacterium tuberculosis* ESX-3 conditional mutant: essentiality and rescue by iron and zinc. *J Bacteriol* 191:6340–6344. <http://dx.doi.org/10.1128/JB.00756-09>.
 20. Tufariello JM, Chapman JR, Kerantzas CA, Wong KW, Vilchère C, Jones CM, Cole LE, Tinaztepe E, Thompson V, Fenyő D, Niederweis M, Ueberheide B, Philips JA, Jacobs WR. 2016. Separable roles for *Mycobacterium tuberculosis* ESX-3 effectors in iron acquisition and virulence. *Proc Natl Acad Sci U S A* 113:E348–E357. <http://dx.doi.org/10.1073/pnas.1523321113>.
 21. Siegrist MS, Steigedal M, Ahmad R, Mehra A, Dragset MS, Schuster BM, Philips JA, Carr SA, Rubin EJ. 2014. Mycobacterial Esx-3 requires multiple components for iron acquisition. *mBio* 5:e01073-14. <http://dx.doi.org/10.1128/mBio.01073-14>.
 22. Jones CM, Niederweis M. 2010. Role of porins in iron uptake by *Mycobacterium smegmatis*. *J Bacteriol* 192:6411–6417. <http://dx.doi.org/10.1128/JB.00986-10>.
 23. Ilghari D, Lightbody KL, Veverka V, Waters LC, Muskett FW, Renshaw PS, Carr MD. 2011. Solution structure of the *Mycobacterium tuberculosis* EsxG–EsxH complex: functional implications and comparisons with other *M. tuberculosis* Esx family complexes. *J Biol Chem* 286:29993–30002. <http://dx.doi.org/10.1074/jbc.M111.248732>.
 24. Hervas-Stubbs S, Majlessi L, Simsova M, Morova J, Rojas MJ, Nouze C, Brodin P, Sebo P, Leclerc C. 2006. High frequency of CD4⁺ T cells specific for the TB10.4 protein correlates with protection against *Mycobacterium tuberculosis* infection. *Infect Immun* 74:3396–3407. <http://dx.doi.org/10.1128/IAI.02086-05>.
 25. Skjot RLV, Oettinger T, Rosenkrands I, Ravn P, Brock I, Jacobsen S, Andersen P. 2000. Comparative evaluation of low-molecular-mass proteins from *Mycobacterium tuberculosis* identifies members of the ESAT-6 family as immunodominant T-cell antigens. *Infect Immun* 68:214–220. <http://dx.doi.org/10.1128/IAI.68.1.214-220.2000>.
 26. Ottenhoff THM, Kaufmann SHE. 2012. Vaccines against tuberculosis: where are we and where do we need to go? *PLoS Pathog* 8:e1002607. <http://dx.doi.org/10.1371/journal.ppat.1002607>.
 27. Sweeney KA, Dao DN, Goldberg MF, Hsu T, Venkataswamy MM, Henaio-Tamayo M, Ordway D, Sellers RS, Jain P, Chen B, Chen M, Kim J, Lukose R, Chan J, Orme IM, Porcelli SA, Jacobs WR. 2011. A recombinant *Mycobacterium smegmatis* induces potent bactericidal immunity against *Mycobacterium tuberculosis*. *Nat Med* 17:1261–1268. <http://dx.doi.org/10.1038/nm.2420>.
 28. Mehra A, Zahra A, Thompson V, Siraengtaksin N, Wells A, Porto M, Köster S, Penberthy K, Kubota Y, Dricot A, Rogan D, Vidal M, Hill DE, Bean AJ, Philips JA. 2013. *Mycobacterium tuberculosis* type VII secreted effector EsxH targets host ESCRT to impair trafficking. *PLoS Pathog* 9:e1003734. <http://dx.doi.org/10.1371/journal.ppat.1003734>.
 29. Copeland NG, Jenkins NA, Court DL. 2001. Recombineering: a powerful new tool for mouse functional genomics. *Nat Rev Genet* 2:769–779. <http://dx.doi.org/10.1038/35093556>.
 30. Datsenko KA, Wanner BL. 2000. One-step inactivation of chromosomal genes in *Escherichia coli* K-12 using PCR products. *Proc Natl Acad Sci U S A* 97:6640–6645. <http://dx.doi.org/10.1073/pnas.120163297>.
 31. Murry JP, Pandey AK, Sassetti CM, Rubin EJ. 2009. Phthiocerol dimycoserolate transport is required for resisting interferon-gamma-independent immunity. *J Infect Dis* 200:774–782. <http://dx.doi.org/10.1086/605128>.
 32. Guo XV, Monteleone M, Klotzsche M, Kamionka A, Hillen W, Braustein M, Ehrh S, Schnappinger D. 2007. Silencing *Mycobacterium smegmatis* by using tetracycline repressors. *J Bacteriol* 189:4614–4623. <http://dx.doi.org/10.1128/JB.00216-07>.
 33. Srivastava S, Ernst Joel D. 2014. Cell-to-cell transfer of *Mycobacterium tuberculosis* antigens optimizes CD4 T cell priming. *Cell Host Microbe* 15:741–752. <http://dx.doi.org/10.1016/j.chom.2014.05.007>.
 34. Rodriguez GM, Voskuil MI, Gold B, Schoolnik GK, Smith I. 2002. *ideR*, an essential gene in *Mycobacterium tuberculosis*: role of IdeR in iron-dependent gene expression, iron metabolism, and oxidative stress response. *Infect Immun* 70:3371–3381. <http://dx.doi.org/10.1128/IAI.70.7.3371-3381.2002>.
 35. Kurthkoti K, Tare P, Paitchowdhury R, Gowthami VN, Garcia MJ, Colangeli R, Chatterji D, Nagaraja V, Rodriguez GM. 2015. The mycobacterial iron-dependent regulator IdeR induces ferritin (bfrB) by alleviating Lsr2 repression. *Mol Microbiol* 98:864–877. <http://dx.doi.org/10.1111/mmi.13166>.
 36. Tullius MV, Harmston CA, Owens CP, Chim N, Morse RP, McMath LM, Iniguez A, Kimmey JM, Sawaya MR, Whitelegge JP, Horwitz MA, Goulding CW. 2011. Discovery and characterization of a unique mycobacterial heme acquisition system. *Proc Natl Acad Sci U S A* 108:5051–5056. <http://dx.doi.org/10.1073/pnas.1009516108>.
 37. Serafini A, Pisu D, Palù G, Rodriguez GM, Manganelli R. 2013. The ESX-3 secretion system is necessary for iron and zinc homeostasis in *Mycobacterium tuberculosis*. *PLoS One* 8:e78351. <http://dx.doi.org/10.1371/journal.pone.0078351>.
 38. Boshoff HI, Solans L, Gonzalo-Asensio J, Sala C, Benjak A, Uplekar S, Rougemont J, Guilhot C, Malaga W, Martín C, Cole ST. 2014. The PhoP-dependent ncRNA Mcr7 modulates the TAT secretion system in *Mycobacterium tuberculosis*. *PLoS Pathog* 10:e1004183. <http://dx.doi.org/10.1371/journal.ppat.1004183>.
 39. Smith I. 2003. *Mycobacterium tuberculosis* pathogenesis and molecular determinants of virulence. *Clin Microbiol Rev* 16:463–496. <http://dx.doi.org/10.1128/CMR.16.3.463-496.2003>.
 40. Cerasi M, Ammendola S, Battistoni A. 2013. Competition for zinc binding in the host-pathogen interaction. *Front Cell Infect Microbiol* 3:108. <http://dx.doi.org/10.3389/fcimb.2013.00108>.
 41. Marcela Rodriguez G, Neyrolles O. 2014. Metallobiology of tuberculosis. *Microbiol Spectrum* 2:3. <http://dx.doi.org/10.1128/microbiolspec.MGM2-0012-2013>.
 42. Siegrist MS, Steigedal M, Ahmad R, Mehra A, Dragset MS, Schuster BM, Philips JA, Carr SA, Rubin EJ. 2014. Mycobacterial Esx-3 requires multiple components for iron acquisition. *mBio* 5:e01073-14. <http://dx.doi.org/10.1128/mBio.01073-14>.
 43. Wagner D, Maser J, Lai B, Cai Z, Barry CE, III, Honer Zu Bentrup K, Russell DG, Bermudez LE. 2005. Elemental analysis of *Mycobacterium avium*-, *Mycobacterium tuberculosis*-, and *Mycobacterium smegmatis*-containing phagosomes indicates pathogen-induced microenvironments within the host cell's endosomal system. *J Immunol* 174:1491–1500. <http://dx.doi.org/10.4049/jimmunol.174.3.1491>.